Like-Charge Attraction at the Nanoscale: Ground-State Correlations and Water Destructuring

Ivan Palaia, Abhay Goyal, Emanuela Del Gado, Ladislav Šamaj, and Emmanuel Trizac*

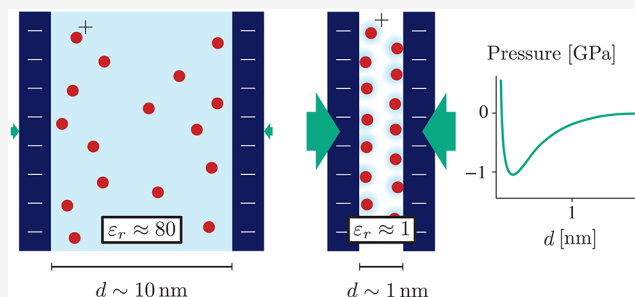Cite This: *J. Phys. Chem. B* 2022, 126, 3143−3149

Read Online

ACCESS | Metrics & More | Article Recommendations

ABSTRACT: Like-charge attraction, driven by ionic correlations, challenges our understanding of electrostatics both in soft and hard matter. For two charged planar surfaces confining counterions and water, we prove that, even at relatively low correlation strength, the relevant physics is the ground-state one, oblivious of fluctuations. Based on this, we derive a simple and accurate interaction pressure that fulfills known exact requirements and can be used as an effective potential. We test this equation against implicit-solvent Monte Carlo simulations and against explicit-solvent simulations of cement and several types of clays. We argue that water destructuring under nanometric confinement drastically reduces dielectric screening, enhancing ionic correlations. Our equation of state at reduced permittivity therefore explains the exotic attractive regime reported for these materials, even in the absence of multivalent counterions.

INTRODUCTION

When two identically charged colloids are immersed in a solvent, their electrostatic interaction is mediated by fluctuating smaller species, such as microions.[1−6] Pioneered by Gouy[7] and Chapman,[8] the statistical treatment of this phenomenon, accounting for thermal fluctuations, is a cornerstone of colloid science and goes by the name of the Poisson−Boltzmann theory.[3,9] Within such a theory, macromolecules bearing a charge of the same sign invariably experience a repulsive force, which provides the Coulombic contribution to the DLVO theory.[3,6] In this framework, electrostatic interactions between similar bodies, of arbitrary geometry, are necessarily repulsive.[10] However, as initially shown by Monte Carlo simulations[11] and integral equations studies,[12] like-charge macromolecules in solution can attract. This counterintuitive phenomenon is the hallmark of electrostatic correlations between ions.[13] Experiments and system-specific simulations proved it to be of paramount importance to explain cement cohesion,[14−16] docking of vesicles,[17,18] and DNA condensation in viruses or cells,[19] as well as the behavior of like-charged mica surfaces,[20] polyelectrolytes,[21] lamellar systems,[22] and lipid bilayers.[23,24] A time-honored rule of thumb is that like-charge attraction requires multivalent counterions.[2,4,9]

From a theoretical standpoint, like-charge attraction provides a complex many-body problem.[25−37] Analytical progress is solely possible in the case where counterions are the only small species present (no added salt) and for simple geometries, e.g., where point ions are confined in water between two planar charged surfaces. These simplifications

maintain the physical relevance: on one hand, confinement often leads to co-ion exclusion and no-salt conditions;[38−40] on the other hand, effective interactions for more complex geometries can be obtained by means of a Derjaguin approximation, once the planar geometry has been solved.[41]
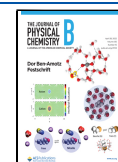
We shall address the problem of understanding the equation of state of a correlated salt-free system with point-like counterions confined between two charged planes: this means describing how the force between planes changes with their distance. The system is represented in the insets of Figure 1, while the rest of the figure shows a sketch of its equation of state, which is nonmonotonic. We argue below that the challenge is to understand the increasing $\mathbb{W}$ branch, while the short distance $\mathbb{IG}$ regime follows from a simple ideal gas argument. More importantly, it is the $\mathbb{W}$ branch that is relevant for a number of applications. While much analytical and computational effort has been invested in this very question and the role of ionic correlations emphasized,[13,25,27,30−37,42−45] most theories fail at accounting for the $\mathbb{W}$ branch.

Our motivation is 3-fold. First, we show that the $\mathbb{W}$ branch is more universal than previously thought and is closely related to the zero-temperature equation of state. Second, elaborating
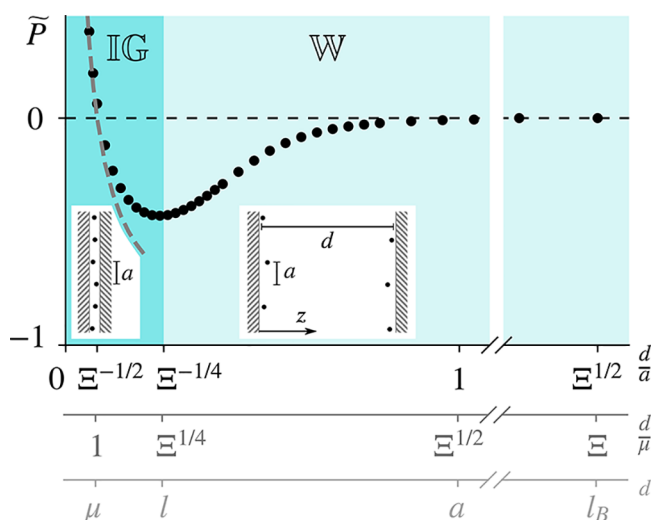
Figure 1. Typical pressure profile between two charged plates at distance d. Here $\Xi = 100$ (Monte Carlo simulations from[43]), but this shape holds whenever an attractive branch exists, meaning $\Xi > 12$. The four relevant length scales are specified below the graph (neglecting numerical prefactors) in units of the Gouy−Chapman length μ and of lateral spacing a. Note the scaling, that helps calculations: $q^2 l_B/a \propto a/\mu \propto (l/\mu)^2 \propto \sqrt{\Xi}$. The cartoons in the insets show microion positions in the slab for the two possible regimes: a short distance "ideal gas" region ($\mathbb{IG}$) for $d < l$ where eq 3 applies (shown by the gray dashed line), and a Wigner region ($\mathbb{W}$) for $d > l$. The system is globally electroneutral.

on a number of exact results, we derive a versatile and accurate equation for the pressure that covers not only the $\mathbb{W}$ branch but also the whole distance range. This equation of state passes the tests of the exact known limiting behaviors while remaining simple, at variance with previous attempts. The third objective of this paper is to investigate a situation where our slab setting is of much relevance, that is under extreme confinement (small interplate distance d, on the order of the size of a water molecule), where the molecular nature of the solvent cannot be disregarded. In line with a number of recent works,[23,46−50] it then becomes essential to account for the destructuring of the water network in the slab, which leads to a dramatic decrease of screening, and a concomitant increase not only of correlations but also of the attractive force between the surfaces. We show that our equation of state applies here in a "vacuum" reformulation that we coin the "locked water picture", and it is directly relevant for clays and cement, where key agents are found in the form of charged nanoplates.[50−52]

■ RESULTS AND DISCUSSION

Relevance of Ground-State Physics. We start by a length scale analysis,[30,37] that provides a fresh overlook. Until stated otherwise, the solvent is considered implicitly by a constant (bulk) permittivity ε_r relative to that of vacuum ε_0 ($\varepsilon_r \simeq 80$ for water); microions are pointlike with valence q. This yields the so-called primitive model, where the Bjerrum length $l_B = e^2/(4\pi\varepsilon_r\varepsilon_0 kT)$ is the distance at which thermal energy kT matches the interaction potential between two elementary charges e. The two plates are modeled as hard surfaces, bearing a homogeneous surface charge density σe, which defines a second important length, named after Gouy[7] and Chapman:[8] $\mu = 1/(2\pi l_B q\sigma)$ is the distance that can be reached with an

energy budget kT, dragging away a single counterion initially at contact with an isolated plate. The so-called coupling parameter, quantifying the importance of ionic correlations, follows as

$$\Xi = \frac{q^2 l_B}{\mu} = 2\pi l_B^2 q^3 \sigma. \tag{1}$$

Comparing electrostatic and thermal energies, Ξ can be viewed as a dimensionless measure of surface charge, inverse permittivity, or, more formally, inverse temperature. $\Xi < 1$ is the regime where the Poisson−Boltzmann theory prevails and the two plates repel, while for $\Xi > 12$, a like-charge attraction sets in.[31] Given that most charged natural or synthetic surfaces have $\sigma < 1$ nm^{-2} and that $l_B \simeq 0.7$ nm in bulk water, monovalent counterions ($q = 1$) lead to small couplings ($\Xi < 4$) and fall under the Poisson−Boltzmann repulsive phenomenology. This explains the rule of thumb alluded to above: attraction, if any, requires $q \geq 2$ and is not possible with monovalent ions. Because of its cubic dependence on valence q, Ξ can reach or significantly exceed a few tens in a wealth of experiments. This is the strong coupling regime we are interested in. Two additional lengths need to be introduced. First, $a = \sqrt{q/\sigma}$ defines the Wigner lattice spacing in the ground state,[53−55] i.e., the distance between neighbor ions when $\Xi \to \infty$ and ions crystallize on each plane. This quantity, which loses relevance in the Poisson−Boltzmann regime, is indicated in Figure 1. It remains essential whenever Ξ is not small. The last player here is the distance l that discriminates between the two regions, $\mathbb{IG}$ and $\mathbb{W}$ in Figure 1. We will see that $l \propto \sqrt{a\mu}$. For large Ξ, the four lengths are in the order $\mu < l < a < l_B$ and their ratios only depend on Ξ, as indicated by the axes in Figure 1.

The two branches in Figure 1 correspond to opposite limiting situations. The left branch has an ideal gas nature[30] and is simple to explain: the two plates are so close that all microions lie in the same plane, and the interior electric field vanishes by symmetry (as a consequence, the potential is quadratic with lateral displacement, a result used below). Since the electric field due to the equal plates also vanishes in the slab, microions become homogeneously distributed along the z coordinate perpendicular to the plate (see Figure 1): their number density reads $n(z) = 2\sigma/(qd)$ by electroneutrality. We then invoke the contact theorem,[5,41,56] a general and exact result relating pressure P to ion density at contact $n(0)$:

$$P = kT(n(0) - 2\pi l_B\sigma^2). \tag{2}$$

This yields a rescaled pressure

$$\widetilde{P} \equiv \frac{P}{2\pi l_B\sigma^2 kT} = \frac{2\mu}{d} - 1. \tag{3}$$

This ideal gas equation of state (dashed gray line in Figure 1) is in good agreement with the pressure measured in the decreasing $\mathbb{IG}$ regime.

The complementary $\mathbb{W}$ branch is more subtle and is fundamentally many-body. We plot in Figure 2 the dimensionless pressure $\widetilde{P}$ as a function of d/a for various couplings Ξ (symbols). This reveals a remarkable collapse: $\widetilde{P}$, that should converge toward the ground state pressure $\widetilde{P}_{gs}$ (black line, worked out in ref 55) only as $\Xi \to \infty$, remains very close to this limiting curve down to unexpectedly small Ξ. Even at low coupling, attraction must then stem from the staggering
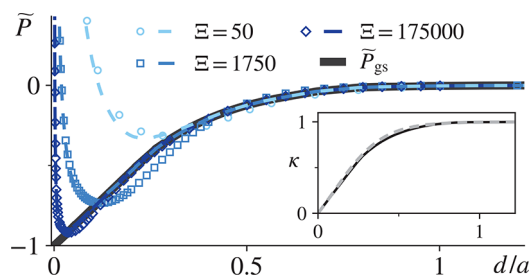
Figure 2. Rescaled pressure versus distance. Monte Carlo simulations from[43] (symbols) are compared to the ground-state pressure $\tilde{P}_{gs}$ ($\Xi \rightarrow \infty$, continuous black line) and to the analytical equation of state (7) and (8) (dashed lines). The inset shows κ versus d/a: the solid line is the exact ground-state value (6), while the dashed line is the analytical approximation (8).

of ions on opposite plates, an ion facing a hole, as in the zero-temperature crystal phase.[53,55] Increasing d, one transitions rather abruptly from the ideal gas branch where interactions are immaterial, to the $\mathbb{W}$ branch that is truly many body. The minimum of the pressure curve, giving the crossover $\mathbb{IG} \leftrightarrow \mathbb{W}$ at $d = l$, is found by equating both limiting results, eq 3 and $\tilde{P}_{gs}$ (we use $\tilde{P}_{gs}+1 \propto d/a$ at small d, as per Figure 2). This yields $l \propto a \, \Xi^{-1/4} \propto \mu \, \Xi^{1/4}$. This exact result, while confirming findings from other methods,[32] disproves the so-called Rouzina−Bloomfield criterion,[25,30] that had $l \propto a$.

Analytical Equation of State. We turn to the second objective of finding an accurate equation of state covering both $\mathbb{IG}$ and $\mathbb{W}$ sectors. Besides ionic positions, the Hamiltonian of the system depends only on the single parameter Ξ,[30] so that the rescaled pressure has two arguments: d and Ξ. We consider two ways of taking the $\Xi \rightarrow \infty$ limit: by keeping d/μ constant or by keeping d/a constant. Since $l/\mu \propto \Xi^{1/4} \rightarrow \infty$, the former magnifies the $\mathbb{IG}$ branch; conversely, since $l/a \propto \Xi^{-1/4} \rightarrow 0$, the latter magnifies the $\mathbb{W}$ branch. We can then write the exact relations:

$$\lim_{\Xi \rightarrow \infty} \widetilde{P}(d, \Xi)|_{d/\mu} = \frac{2\mu}{d} - 1; \tag{4}$$

$$\lim_{\Xi \rightarrow \infty} \widetilde{P}(d, \Xi)|_{d/a} = \widetilde{P}_{gs}(d) \tag{5}$$

where $\tilde{P}_{gs}$ varies over distances of scale a, as shown in Figure 2. In eq 4, the large Ξ limit is taken at fixed d/μ while it is the ratio d/a that is held fixed in eq 5. Statement 4 indicates a flat, ideal gas profile on a scale μ (see eq 3). This occurs because the energy cost for an ion to move from one plate to the other is $\Delta E \propto kT \, l_B \, d^2/a^3 \propto (d/\mu)^2 \, \Xi^{-1/2} \rightarrow 0$. Statement 5, instead, expresses the constraint that on a scale a any trace of fluctuations disappears and the ground state pressure is recovered. We will demand that an approximate pressure fulfill both constraints, in addition to being trustworthy for as wide a range of Ξ values as possible.

To proceed, it is useful to understand which ground-state properties are inherited by the finite-Ξ system. What is common between infinite and finite (but nonsmall) Ξ regimes is the local electric field acting on an ion. The reason is that the extent of allowed fluctuations along z is always much smaller than a. For an isolated ion on a single plate (the other plate being at infinite d, screened by its own ions), this field is attractive, given by $E_0 = e\sigma/(2\varepsilon_0\varepsilon_r)$. In the ground state as well as at finite Ξ, an ion sees similar environments: a layer of ions close to the same plate that do not create any local field along z

and a layer of ions on the opposite plate that contribute to renormalize the bare field E_0 by a factor κ, which depends on d/a. We have just argued that $\kappa \rightarrow 1$ for $d/a \rightarrow \infty$, while $\kappa \rightarrow 0$ for $d/a \rightarrow 0$ (where one must recover the ideal gas picture, i.e. a null electric field). More generally, the following simple mechanical argument relates κ to $\tilde{P}_{gs}$. In the ground state, each ion at contact with the plate pushes on it with a force κeqE_0; there are σ/q ions per unit surface, so the repulsive force per unit surface is $\kappa e\sigma E_0$. At the same time, the plate feels an attractive force due to the presence of the ion layer and of the other plate: their overall charge density is σe, and so is the charge of the initial plate, modulo a sign, so that the force per unit surface is $-(\sigma e)^2/(2\varepsilon_0\varepsilon_r) = -e\sigma E_0$. The total force acting on the plate is then the sum of these contact and electrostatic components, i.e., $P_{gs} = (\kappa - 1)e\sigma E_0 = (\kappa - 1)\sigma^2 e^2/(2\varepsilon_0\varepsilon_r)$. In dimensionless form:

$$\kappa = 1 + \widetilde{P}_{gs}. \tag{6}$$

This relation can be viewed as a contact-value theorem at $T = 0$. Exact in the ground state, we will show that it is an excellent approximation even at finite Ξ.

Since the ionic layer thickness is always much smaller than the interion distance a,[43] the ionic profile follows from a single particle argument in the effective potential $\kappa qeE_0z = kT\kappa z/\mu$: thus $n(z) \propto e^{-\kappa z/\mu}$. We normalize n by imposing electroneutrality (i.e., $\int_0^d n(z) \, dz = 2\sigma/q$) and, using once more the contact theorem (2), we obtain the equation of state

$$\widetilde{P} = \kappa \frac{1 + e^{-\kappa d/\mu}}{1 - e^{-\kappa d/\mu}} - 1, \tag{7}$$

which exhibits a dependence on the two length scales μ and a (through κ). Such a functional form coincides with the leading order of a large-Ξ expansion in the Wigner Strong Coupling approach.[43] What remains is to find an expression for $\kappa = 1 + \tilde{P}_{gs}$. It was shown that $\tilde{P}_{gs} \sim -3 \exp(-\alpha d/a)$ for $d \gg a$, with $\alpha = 4\pi/(3^{1/4}\sqrt{2}) \simeq 6.75$.[55] Given that $\kappa \rightarrow 0$ for $d \ll a$, the simplest form compatible with the two limits is

$$\kappa = 1 - \frac{3}{2 + e^{\alpha d/a}}. \tag{8}$$

This is compared with eq 6 in the inset of Figure 2.

Equation of state 7, supplemented with (8), is our jackknife pressure. It is not exact, but it is the only available simple pressure compatible with exact limiting results, such as (4) and (5). It complies with the energetic attraction/entropic repulsion phenomenology put forward in earlier works, e.g. ref 13. Figure 2 (dashed lines) illustrates its good accuracy down to $\Xi = 50$ when compared to Monte Carlo results (symbols), thus confirming the relevance of ground-state physics at surprisingly low Ξ.

Water Destructuring under Confinement. The previous discussion holds within the (solvent implicit) primitive model, where water enters the description only through its permittivity ε_r. It is customary to take $\varepsilon_r = 80$, the bulk value. Yet, in situations of strong confinement, when d becomes comparable to the size of water molecules, this choice is questionable, if not misguided. Recent works indeed point to the fact that water organization is strongly affected at small d, with a freezing of orientational degrees of freedom: this decreases its effective ε_r.[23,46−50] One might believe that these considerations ruin implicit-water approaches, and in particular

the primitive model. We show evidence that this is not the case.

Recently, pure water confined between neutral surfaces below 2 nm was shown to exhibit a relative permittivity between 1 and 4, depending on d.[47] This came as a confirmation of theoretical results that anticipated a drastic decrease in the component of the dielectric tensor perpendicular to the confining surfaces.[46,49] A complete understanding of how confinement and environment affects ε_r is still lacking, but we speculate that for strongly charged surfaces and in the presence of ions, water mobility is suppressed even more strongly, resulting in a permittivity close to that of vacuum. We argue that decreasing d, the number of counterions in the slab remains fixed by electroneutrality, while water content diminishes. Water is then dominantly immobilized in hydration layers around counterions, and cannot screen Coulombic interactions like it does in the bulk. This behavior was confirmed in simulations,[50] where qualitative measurements of both components of the dielectric tensor showed a drastic decrease. As we seek to understand attraction from first-principles only, we make the assumption that water molecules in the slab are so few that none of them is free: this leads to the crude approximation $\varepsilon_r \to 1$, for d smaller than a couple nanometers. We coin the resulting suppressed-permittivity primitive model the "locked water" model:[50] in it, l_B is renormalized, substituted by $l_B^{\text{locked}} = 80 l_B$ in all expressions. Besides dampening van der Waals interactions,[23,57] this enormously increases coupling to $\Xi^{\text{locked}} = 80^2 \Xi$ and drives a massive increase in attraction; this is consistent with what proposed in ref 48, where pressure between confined decanol bilayers was shown to be described by a larger coupling than expected. A consequence is that for small enough d, a very small surface charge σ becomes sufficient to lead to attraction even with monovalent ions ($q = 1$), unlike previously thought: the condition for attraction mentioned above, now $\Xi^{\text{locked}} > 12$, is met for σq^3 just above 0.03 nm^{-2}, at room temperature.

The equation of state, (7) and (8), within the "locked water" primitive model can be tested against water-explicit simulations. We take as sample systems cement and clays, whose effective interactions at the nanoscale have puzzled scientists for decades. Figure 3 compares different models for calcium silicate hydrate (C−S−H), the main binding agent of cement:[14] these include fully atomistic simulations[51] and two coarse-grained models,[50] where particles are Lennard-Jones spheres and the dielectric properties of a water molecule emerge either from a point dipole (dipolar model, DM) or from point partial charges (SPC/E model[58]). Analogously, Figure 4 compares dipolar model simulations of clays from ref 52 with eqs 7 and 8 for "locked water". In both figures, curves are shifted horizontally to account for different ion sizes and different descriptions of the walls. This shift is not the result of a fit and is determined by parameters used in simulations for wall thickness or ion diameter. Ambiguities resulting from surface roughness or soft potentials are small and have been resolved by checking for the positions of the two furthermost peaks of the counterion density. In addition, while in simulations of cement the high electric fields involved, at any d, squeeze counterions against the walls and expel half of their solvation shell,[50] the lower surface charges of clays are not always sufficient to quench hydration: for clays, the shape of the solvation shells is known to drastically depend on distance,
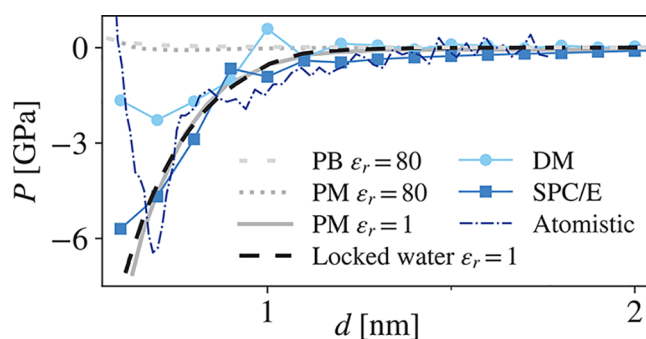

Figure 3. Interplate pressure in C−S−H systems, where $\sigma = 3$ nm^{-2} and ions are Ca^{2+}. In blue tones, water-explicit MD simulations from refs 50 and 51 for the dipolar model (DM), SPC/E, and fully atomistic. In gray, MD simulations of the primitive model (PM), at different ε_r, and Poisson−Boltzmann (PB) results. In dashed black, eqs 7 and 8 at $\varepsilon_r = 1$. Curves are shifted horizontally, using SPC/E as reference, to account for different sizes and descriptions of the ions and the plate surface.
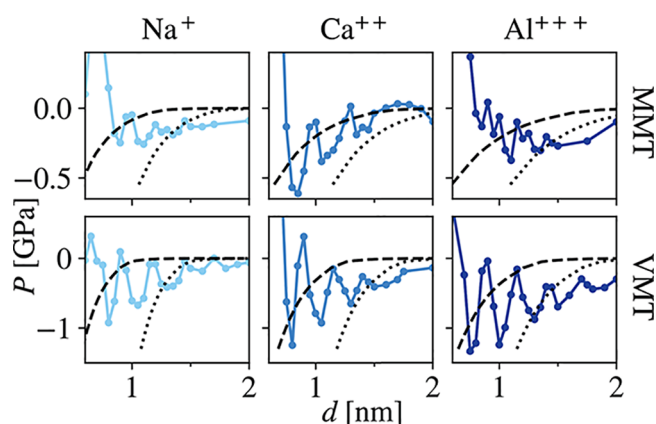

Figure 4. Pressure predictions for clays. Above, montmorillonite (MMT, $\sigma = 0.75$ nm^{-2}); below, vermiculite (VMT, $\sigma = 1.5$ nm^{-2}). Valence q increases columnwise, from 1 to 3. Coupling Ξ^{locked} varies accordingly, from 15000 (top left) to 820000 (bottom right). Circles show dipolar model MD simulations from ref 52 while black lines are from eqs 7 and 8 at $\varepsilon_r = 1$. A shift accounts, as in Figure 3, for finite ion and wall sizes. In particular, the dotted curve assumes fully hydrated ions, while the dashed one a halved hydration shell. The "locked water" model predicts a pressure between the two black curves.

incidentally causing swelling.[59,60] This is why in Figure 4 we include two analytical curves, shifted by two water molecule diameters from one another. The theoretical prediction lies between the two curves.

Figure 3 shows that eqs 7 and 8 within our "locked water" picture explain results from all three computational models. In particular, the primitive model at $\varepsilon_r = 80$ catastrophically misses the simulated pressure curves by 2 orders of magnitude, whereas our "locked water" picture captures both their magnitude and qualitative behavior. The Poisson−Boltzmann approximation (DLVO),[5] as mentioned, can only predict repulsion[10] and is completely wrong. Figure 4 shows similar results. Here, the pressure oscillations observed are fingerprints of the water diameter ($\simeq 0.3$ nm) and a full account of these would require a finer molecular description; nonetheless, general trends and magnitudes are well captured. This is not trivial, as state-of-the-art implicit-solvent theoretical models involve $\varepsilon_r = 80$, and miss, again, even the order of magnitude of

the pressure. Moreover, we explain the observed attraction in the presence of monovalent ions (Na^+), recently reported also for lipid bilayers.[23]

In both Figures 3 and 4, the dramatic increase from the bulk Ξ to Ξ^{locked} decreases the crossover length l by a factor $\sqrt{80} \simeq 9$. This extends the relevance of the $\mathbb{W}$ branch and contributes to masking the $\mathbb{IG}$ regime. In simulations, the steep rise at small distances is indeed not of electrostatic origin, but due to steric ion-wall repulsion. In general, in real systems, the $\mathbb{IG}$ branch and possibly the initial part of the $\mathbb{W}$ branch will be masked by other additive components of the pressure, such as hydration or surface—surface contact forces. These short-range forces, typically described at a phenomenological level,[41] are not accounted for in our first-principles model. However, the many experimental and numerical observations of like-charge attraction under confinement, as well as Figure 3 and 4, suggest that they are unlikely to screen the longer-range attractive branch of the electrostatic correlation pressure.

Charge regulation and surface charge heterogeneity are not included explicitly in our model. These aspects might play a role in determining the strength of attraction. For instance, pH is known to drastically regulate charge in cement, as the hydration reaction proceeds.[50,61,62] A relevant observation is that, in the ground-state picture that inspires our equation of state, ions are immobilized on the surface, as also observed in simulations.[50] This is effectively equivalent to having counterions chemically bound to the surface, assuming that they produce a localized excess positive charge on the negative plate. In sum, the only thing that matters to have correlation-induced attraction is a (staggered) nonuniform charge distribution on the plates, be it from localized chemically bound charges or from ions dwelling at the interfaces. Consistent with this scenario, charge regulation with discrete titration sites has recently been suggested to even increase attraction at the nanoscale.[63]

CONCLUSIONS

We have derived a robust, simple, and accurate equation of state for strongly charged plates with ions and water in between. This jackknife pressure, eqs 7 and 8, satisfies the exact requirements, both at the scale of the Gouy—Chapman length μ, eq 4, and at that of the Wigner spacing a, eq 5. This clarifies the rather elusive primitive model phenomenology, showing that ground state physics, a basic ingredient of our equation of state, is unexpectedly relevant even at moderate coupling. The origin of attraction must then lie in the fact that ions dwelling next to one plane anticorrelate with those next to the other plane, reminiscent of the staggered lattice formed at zero temperature.

We have shown that upon renormalizing the Bjerrum length to consider its *vacuum* counterpart l_B^{locked}, it becomes possible, with an implicit-solvent approach, to explain explicit-water results under strong confinement. This "locked water" view predicts in particular the possibility of attractive effective interactions with monovalent counterions, at variance with common belief, but explaining the behavior of clays and lipid bilayers.[23] Using the present jackknife equation of state 7 and 8 as an effective potential to upscale coarse-grained simulations is a promising avenue.

AUTHOR INFORMATION

Corresponding Author

Emmanuel Trizac − *Université Paris-Saclay, CNRS, LPTMS, 91405 Orsay, France*; Email: emmanuel.trizac@universite-paris-saclay.fr

Authors

Ivan Palaia − *Institute of Science and Technology Austria, 3400 Klosterneuburg, Austria*; ⓘ orcid.org/0000-0002-8843-9485

Abhay Goyal − *Department of Physics, Institute for Soft Matter Synthesis and Metrology, Georgetown University, Washington, D.C. 20057, United States*; ⓘ orcid.org/0000-0002-0587-2145

Emanuela Del Gado − *Department of Physics, Institute for Soft Matter Synthesis and Metrology, Georgetown University, Washington, D.C. 20057, United States*; ⓘ orcid.org/0000-0002-8340-0290

Ladislav Šamaj − *Institute of Physics, Slovak Academy of Sciences, 84511 Bratislava, Slovakia*

Complete contact information is available at:
https://pubs.acs.org/10.1021/acs.jpcb.2c00028

Notes

The authors declare no competing financial interest.

REFERENCES

(1) Hansen, J.-P.; Löwen, H. Effective interactions between electric double layers. *Annu. Rev. Phys. Chem.* **2000**, *51*, 209.

(2) Belloni, L. Colloidal interactions. *J. Phys.: Condens. Matt.* **2000**, *12*, R549.

(3) Hunter, R. J. *Foundations of Colloid Science*, 2nd ed.; Oxford University Press: 2001.

(4) Levin, Y. Electrostatic correlations: from plasma to biology. *Rep. Prog. Phys.* **2002**, *65*, 1577−1632.

(5) Andelman, D., Introduction to electrostatics in soft and biological matter. In *Soft Condensed Matter Physics in Molecular and Cell Biology*, edited by Poon, W., Andelman, D., Eds.; Taylor and Francis; 2006; pp 97−122.

(6) Zhao, K.; Mason, T. G. Assembly of colloidal particles in solution. *Rep. Prog. Phys.* **2018**, *81*, 126601.

(7) Gouy, M. Sur la constitution de la charge électrique à la surface d'un électrolyte. *Journal de Physique Théorique et Appliquée* **1910**, *9*, 457.

(8) Chapman, D. L. A contribution to the theory of electro-capillarity. *London, Edinburgh, and Dublin Philosophical Magazine and Journal of Science* **1913**, *25*, 475.

(9) Messina, R. Electrostatics in soft matter. *J. Phys.: Condens. Matter* **2009**, *21*, 113102.

(10) Neu, J. C. Wall-mediated forces between like-charged bodies in an electrolyte. *Phys. Rev. Lett.* **1999**, *82*, 1072.

(11) Guldbrand, L.; Jönsson, B.; Wennerström, H.; Linse, P. Electrical double layer forces. A Monte Carlo study. *J. Chem. Phys.* **1984**, *80*, 2221.

(12) Kjellander, R.; Marčelja, S. Correlation and image charge effects in electrical double layers. *Chem. Phys. Lett.* **1984**, *112*, 49.

(13) Jönsson, B.; Wennerström, H. Ion-ion correlations in liquid dispersions. *J. Adhes.* **2004**, *80*, 339.

(14) Pellenq, R. J.-M.; Van Damme, H. Why Does Concrete Set?: The Nature of Cohesion Forces in Hardened Cement-Based Materials. *MRS Bull.* **2004**, *29*, 319.

(15) Pellenq, R.-M.; Caillol, J.; Delville, A. Electrostatic Attraction between Two Charged Surfaces: A (N, V, T) Monte Carlo Simulation. *J. Phys. Chem. B* **1997**, *101*, 8584.

(16) Plassard, C.; Lesniewska, E.; Pochard, I.; Nonat, A. Nanoscale experimental investigation of particle interactions at the origin of the cohesion of cement. *Langmuir* **2005**, *21*, 7263.

(17) Komorowski, K.; Salditt, A.; Xu, Y.; Yavuz, H.; Brennich, M.; Jahn, R.; Salditt, T. Vesicle adhesion and fusion studied by small-angle X-ray scattering. *Biophys. J.* **2018**, *114*, 1908.

(18) Komorowski, K.; Schaeper, J.; Sztucki, M.; Sharpnack, L.; Brehm, G.; Köster, S.; Salditt, T. Vesicle adhesion in the electrostatic strong-coupling regime studied by time-resolved small-angle X-ray scattering. *Soft Matter* **2020**, *16*, 4142.

(19) Bloomfield, V. A. Condensation of DNA by multivalent cations: Considerations on mechanism. *Biopolymers* **1991**, *31*, 1471.

(20) Kékicheff, P.; Marčelja, S.; Senden, T.; Shubin, V. Charge reversal seen in electrical double layer interaction of surfaces immersed in 2:1 calcium electrolyte. *J. Chem. Phys.* **1993**, *99*, 6098.

(21) Angelini, T. E.; Liang, H.; Wriggers, W.; Wong, G. C. Like-charge attraction between polyelectrolytes induced by counterion charge density waves. *Proc. Natl. Acad. Sci. U.S.A.* **2003**, *100*, 8634.

(22) Khan, A.; Jönsson, B.; Wennerström, H. Phase equilibria in the mixed sodium and calcium di-2- ethylhexylsulfosuccinate aqueous system. An illustration of repulsive and attractive double-layer forces. *J. Phys. Chem.* **1985**, *89*, 5180.

(23) Mukhina, T.; Hemmerle, A.; Rondelli, V.; Gerelli, Y.; Fragneto, G.; Daillant, J.; Charitat, T. Attractive Interaction between Fully Charged Lipid Bilayers in a Strongly Confined Geometry. *J. Phys. Chem. Lett.* **2019**, *10*, 7195.

(24) Fink, L.; Steiner, A.; Szekely, O.; Szekely, P.; Raviv, U. Structure and Interactions between Charged Lipid Membranes in the Presence of Multivalent Ions. *Langmuir* **2019**, *35*, 9694.

(25) Rouzina, I.; Bloomfield, V. Macroion attraction due to electrostatic correlation between screening counterions. 1. Mobile surface-adsorbed ions and diffuse ion cloud. *J. Phys. Chem.* **1996**, *100*, 9977.

(26) Allahyarov, E.; D'Amico, I.; Löwen, H. Attraction between Like-Charged Macroions by Coulomb Depletion. *Phys. Rev. Lett.* **1998**, *81*, 1334.

(27) Shklovskii, B. Screening of a macroion by multivalent ions: Correlation-induced inversion of charge. *Phys. Rev. E* **1999**, *60*, 5802.

(28) Levin, Y. When do like charges attract? *Physica A* **1999**, *265*, 432.

(29) Lau, A.; Levine, D.; Pincus, P. Novel electrostatic attraction from plasmon fluctuations. *Phys. Rev. Lett.* **2000**, *84*, 4116.

(30) Netz, R. Electrostatistics of counter-ions at and between planar charged walls: From Poisson-Boltzmann to the strong-coupling theory. *Eur. Phys. J. E* **2001**, *5*, 557.

(31) Moreira, A.; Netz, R. Simulations of counterions at charged plates. *Eur. Phys. J. E* **2002**, *8*, 33.

(32) Chen, Y.-G.; Weeks, J. Local molecular field theory for effective attractions between like charged objects in systems with strong Coulomb interactions. *Proc. Natl. Acad. Sci. U.S.A.* **2006**, *103*, 7560.

(33) Santangelo, C. D. Computing counterion densities at intermediate coupling. *Phys. Rev. E* **2006**, *73*, 041512.

(34) Pegado, L.; Jönsson, B.; Wennerström, H. Ion-ion correlation attraction in a molecular solvent. *J. Chem. Phys.* **2008**, *129*, 184503.

(35) Hatlo, M. M.; Lue, L. A field theory for ions near charged surfaces valid from weak to strong couplings. *Soft Matter* **2009**, *5*, 125.

(36) Bakhshandeh, A.; dos Santos, A. P.; Levin, Y. Weak and strong coupling theories for polarizable colloids and nanoparticles. *Phys. Rev. Lett.* **2011**, *107*, 107801.

(37) Naji, A.; Kanduč, M.; Forsman, J.; Podgornik, R. Perspective: Coulomb fluids—Weak coupling, strong coupling, in between and beyond. *J. Chem. Phys.* **2013**, *139*, 150901.

(38) Yang, K.-L.; Yiacoumi, S.; Tsouris, C. Monte Carlo simulations of electrical double-layer formation in nanopores. *J. Chem. Phys.* **2002**, *117*, 8499.

(39) Hishida, M.; Nomura, Y.; Akiyama, R.; Yamamura, Y.; Saito, K. Electrostatic double-layer interaction between stacked charged bilayers. *Phys. Rev. E* **2017**, *96*, 040601.

(40) Tournassat, C.; Bourg, I.; Holmboe, M.; Sposito, G.; Steefel, C. Molecular Dynamics Simulations of Anion Exclusion in Clay Interlayer Nanopores. *Clays and Clay Minerals* **2016**, *64*, 374.

(41) Israelachvili, J. N. *Intermolecular and Surface Forces*, 3rd ed.; Elsevier Inc.: 2011.

(42) Kanduč, M.; Trulsson, M.; Naji, A.; Burak, Y.; Forsman, J.; Podgornik, R. Weak- and strong-coupling electrostatic interactions between asymmetrically charged planar surfaces. *Phys. Rev. E* **2008**, *78*, 061105.

(43) Šamaj, L.; Trulsson, M.; Trizac, E. Strong-coupling theory of counterions between symmetrically charged walls: From crystal to fluid phases. *Soft Matter* **2018**, *14*, 4040.

(44) Grønbech-Jensen, N.; Mashl, R. J.; Bruinsma, R. F.; Gelbart, W. M. Counterion-Induced Attraction between Rigid Polyelectrolytes. *Phys. Rev. Lett.* **1997**, *78*, 2477.

(45) Linse, P.; Lobaskin, V. Electrostatic attraction and phase separation in solutions of like-charged colloidal particles. *Phys. Rev. Lett.* **1999**, *83*, 4208.

(46) Schlaich, A.; Knapp, E. W.; Netz, R. R. Water Dielectric Effects in Planar Confinement. *Phys. Rev. Lett.* **2016**, *117*, 048001.

(47) Fumagalli, L.; Esfandiar, A.; Fabregas, R.; Hu, S.; Ares, P.; Janardanan, A.; Yang, Q.; Radha, B.; Taniguchi, T.; Watanabe, K.; Gomila, G.; Novoselov, K. S.; Geim, A. K. Anomalously low dielectric constant of confined water. *Science* **2018**, *360*, 1339.

(48) Schlaich, A.; Dos Santos, A. P.; Netz, R. R. Simulations of Nanoseparated Charged Surfaces Reveal Charge- Induced Water Reorientation and Nonadditivity of Hydration and Mean-Field Electrostatic Repulsion. *Langmuir* **2019**, *35*, 551.

(49) Loche, P.; Ayaz, C.; Wolde-Kidan, A.; Schlaich, A.; Netz, R. R. Universal and Nonuniversal Aspects of Electrostatics in Aqueous Nanoconfinement. *J. Phys. Chem. B* **2020**, *124*, 4365.

(50) Goyal, A.; Palaia, I.; Ioannidou, K.; Ulm, F.-J.; van Damme, H.; Pellenq, R.; Trizac, E.; Del Gado, E. The physics of cement cohesion. *Sci. Adv.* **2021**, *7*, eabg5882.

(51) Masoumi, S.; Valipour, H.; Abdolhosseini Qomi, M. J. Intermolecular Forces between Nanolayers of Crystalline Calcium-Silicate-Hydrates in Aqueous Medium. *J. Phys. Chem. C* **2017**, *121*, 5565.

(52) Carrier, B. Influence of water on the short-term and long-term mechanical properties of swelling clays: experiments on self-supporting films and molecular simulations. Ph.D. Thesis; Paris-Est University: 2014.

(53) Goldoni, G.; Peeters, F. Stability, dynamical properties, and melting of a classical bilayer Wigner crystal. *Phys. Rev. B* **1996**, *53*, 4591.

(54) Lobaskin, V.; Netz, R. Ground state structure and interactions between dimeric 2D Wigner crystals. *EPL* **2007**, *77*, 38003.

(55) Šamaj, L.; Trizac, E. Critical phenomena and phase sequence in a classical bilayer Wigner crystal at zero temperature. *Phys. Rev. B* **2012**, *85*, 205131.

(56) Henderson, D.; Blum, L.; Lebowitz, J. An exact formula for the contact value of the density profile of a system of charged hard spheres near a charged wall. *J. Electroanal. Chem.* **1979**, *102*, 315.

(57) Parsegian, V. A. *Van Der Waals Forces: A Handbook for Biologists, Chemists, Engineers, and Physicists*; Cambridge University Press: 2005.

(58) Berendsen, H.; Grigera, J.; Straatsma, T. The missing term in eective pair potentials. *J. Phys. Chem.* **1987**, *91*, 6269.

(59) Hensen, E. J. M.; Smit, B. Why Clays Swell, The. *J. Phys. Chem. B* **2002**, *106*, 12664.

(60) Brochard, L. Swelling of Montmorillonite from Molecular Simulations: Hydration Diagram and Confined Water Properties. *J. Phys. Chem. C* **2021**, *125*, 15527.

(61) Labbez, C.; Jönsson, B.; Pochard, I.; Nonat, A.; Cabane, B. Surface charge density and electrokinetic potential of highly charged minerals: Experiments and Monte Carlo simulations on calcium silicate hydrate, Journal of. *Physical Chemistry B* **2006**, *110*, 9219.

(62) Labbez, C.; Pochard, I.; Jönsson, B.; Nonat, A. C−S−H/ solution interface: Experimental and Monte Carlo studies. *Cem. Concr. Res.* **2011**, *41*, 161.

(63) Curk, T.; Luijten, E. Charge Regulation Effects in Nanoparticle Self-Assembly. *Phys. Rev. Lett.* **2021**, *126*, 138003.